Electronic Supplementary Information:

Decoupling the Metal—Insulator Transition Temperature and Hysteresis of of VO_2 Using Ge Alloying and Oxygen Vacancies

Parker Schofield,[a,b¶] Erick J. Braham,[a,b¶] Baiyu Zhang,[b¶] Justin L. Andrews,[a,b] Hayley Drozdick,[a] Dexin Zhao,[b] Wasif Zaheer, [a,b] Rebeca Gurrola,[b] Kelvin Xie,[b] Patrick J. Shamberger,[b] Xiaofeng Qian,[b,c*] Sarbajit Banerjee[a,b*]

[a]Department of Chemistry, Texas A&M University, College Station, TX 77843, USA

[b]Department of Materials Science and Engineering, Texas A&M University, College Station, TX 77843, USA

[c]Department of Electrical and Computer Engineering, Texas A&M University, College Station, TX 77843, USA

[¶]These authors contributed equally to this work

*E-mail: feng@tamu.edu banerjee@chem.tamu.edu

Materials and Methods

Undoped VO_2 nanowires

VO_2(B) nanowires were obtained by modification of a previously published synthesis.[1] Briefly, bulk V_2O_5 (Sigma Aldrich, 99.99%) powder, 14 mL of deionized water (ρ = 18 MΩcm^{-1}, Barnstead International NANOpure Diamond system), and 4 mL of 2-propanol were sealed in a 23 mL capacity polytetrafluoroethylene (PTFE)-lined stainless steel autoclave (Parr) and heated at 250°C for 48 h. The autoclave was allowed to cool to room temperature autogenously. Blue/black powder was obtained by vacuum filtration and allowed to dry under ambient conditions for 12 h. The dried powder was annealed in a tube furnace under flowing argon gas at 550°C for 12 h to ensure all VO_2 present was M1 in phase.

Solid-state Synthesis of $Ge_xV_{1-x}O_2$

$Ge_xV_{1-x}O_2$ powders were synthesized according to a traditional ceramic method. Stoichiometric amounts of bulk GeO_2 (Aldrich, 99.99%) powder and hydrothermally prepared VO_2(B) nanowires were ground in a mortar and pestle and sealed in a fused silica ampoule under vacuum. The sealed ampoule was heated at 900°C for 96 h and quenched to room temperature in a water bath (the mass yield is greatly increased contrasting 48 and 96 h samples). The higher reaction time helps in dissolution of incorporation of GeO_2 and homogeneous Ge incorporation in VO_2. The powder obtained from the reaction was re-ground using a mortar and pestle and sealed in a fused silica ampoule and heated at 900°C for another 96 h to achieve a phase-pure product. The as-obtained powders were examined in subsequent measurements without further purification.

Hydrothermal Synthesis of $Ge_xV_{1-x}O_2$

Vanadic acid (HVO_3, 0.4 M) was prepared immediately prior to each synthesis by flowing aqueous solutions of dissolved sodium metavanadate ($NaVO_3$, 0.4 M, Alfa Aesar, 96%) through an Amberlite IRN-77 (Alfa Aesar) styrene-divinylbenzene acidic cation exchange column. In a 23 mL PTFE liner, the prepared HVO_3 solution (8 mL) was combined with 2-propanol (IPA, 6-8 mL, Fisher Chemical, 99.5%) used as a reducing agent and water (2-0 mL) to achieve a final volume of 16 mL. Germanium oxide (10—50 mg, Aldrich, 99.99%) was added to this solution and the PTFE cup was sealed with a PTFE lid.

The sealed PTFE liners were inserted into sealed 23 mL steel autoclaves and allowed to react in an oven heated to 250°C for 72 h. The autoclaves were then removed from the oven, air-cooled, and the samples were removed and centrifuged at 8700 rpm for 9 min. The centrifuged samples were then rinsed with water and centrifuged again at 8700 rpm for 9 min. The process of rinsing and centrifuging the sample was then repeated twice using 2-propanol. The sample was then air-dried and annealed under flowing argon at 550°C in a tube furnace for 6 h. Samples were analyzed *via* powder X-ray diffraction and differential scanning calorimetry (techniques detailed below).

Scanning Electron Microscopy (SEM)

SEM images were collected using a Tescan LYRA-3 instrument equipped with an Oxford energy dispersive X-ray spectroscopy (EDS), operating at accelerating voltages in the range of 5—15 kV

Transmission Electron Microscopy (TEM)

TEM was used to investigate the morphology and elemental composition of hydrothermally prepared $Ge_{0.1}V_{0.9}O_2$. Composition mapping of $Ge_{0.1}V_{0.9}O_2$ was performed using scanning transmission electron microscopy (STEM) energy dispersive spectroscopy (EDS) mapping on a FEI Tecnai G2 F20 Super-Twin FE-TEM instrument operated at 200 kV.

Powder X-ray Diffraction

Powder X-ray diffraction (XRD) patterns were collected in Bragg-Brentano geometry on a D8-focus diffractometer (Cu Kα radiation; λ = 1.5418Å; 40 kV voltage; 25 mA current). All Rietveld refinements were performed using GSAS-II.[2] All crystal structure renditions were prepared using the Vesta III software suite (JP-Minerals).[3,4]

Differential Scanning Calorimetry

Differential scanning calorimetry (DSC) was conducted on 5—10 mg samples using a Q2000 model calorimeter from TA Instruments. DSC measurements were calibrated using an indium enthalpy standard accurate to ± 0.1°C. Temperatures were scanned at 15°C/min unless indicated otherwise.

Optical Microscopy

$Ge_xV_{1-x}O_2$ powders were ultrasonicated in high-purity ethanol and a drop of the resulting suspension was cast onto a glass coverslip. After leaving time for the ethanol to evaporate, the particles were redistributed by passing a second coverslip across the sample. This yielded loose adherence of the sample to the glass. Optical microscopy was conducted on an Olympus BX-53 polarized light microscope and an Olympus UC30 color CCD camera for image capture. Using bright-field-reflected, unpolarized white light, exposure was manually selected and sustained throughout image capture. Temperature was controlled with a Linkham LTS120 Peltier temperature stage with a range of 20−100 °C, accurate to ±0.1°C. Blue-shifted reflected light in the 600—800 nm wavelength range was used as a diagnostic of the metal-to-insulator transition.[5]

Computational methods

The defect formation energies were calculated using first-principles DFT[6,7] as implemented in the Vienna Ab initio Simulation Package (VASP).[8] The Perdew-Burke-Ernzerhof (PBE)[9] form of exchange-correlation functional within the generalized gradient approximation (GGA)[10] and a plane wave basis set with a 533 eV energy cutoff were employed for VASP calculations. A Hubbard parameter *U* of 3.4 eV was applied, considering the strongly correlated 3d electrons of vanadium. Spin polarization was considered for all the defect calculations. The defect structural optimization and electronic relaxation were calculated using a Γ-centered Monkhorst-Pack[11] k-point sampling grid of 3×3×3, with a supercell containing 96 atoms to mimic the defect dilute limit. Finally, an energy correction was applied to the formation energy to address the spurious image charge interaction that arises from the finite supercell formalism.[12]

In order to reproduce the experimental V—V bond dimerization in M1 VO_2, we further employ the HSE06 hybrid functional[13] to calculate the lattice parameters and bond lengths with and without Ge dopants in a VO_2 supercell, containing 96 atoms. Spin polarization is also considered in order to deal with the unpaired electrons induced by the dopant. As shown in **Table S3**, the HSE06 functional can better capture the lattice parameters and V—V dimerization, as compared to the PBE functional.

Neutron Activation Analysis

Mass fractions of V and O were determined by 14-MeV fast neutron activation analysis[14] using the direct comparator method to afford a high degree of accuracy to the measurements.[15] The determination of V utilized the $^{51}V(n,p)^{51}Ti$ reaction. The determination of O used the $^{16}O(n,p)^{16}N$ reaction.[16]

Aliquots of approx. 100 mg of each sample were weighed and heat-sealed in pre-cleaned low-density polyethylene irradiation vials under an argon atmosphere. Vanadium calibrators were prepared from dried aliquots of high-purity V_2O_5, in the same manner as the samples. Polyethylene cylinders doped at various levels with TiO_2 were used as oxygen calibrators.[15] Empty irradiation vials were included to assess the blank contributions of the sample packaging.

The sample aliquots, calibrators, and blanks were irradiated using a Kaman A-711 neutron generator at a nominal 14-MeV neutron fluence rate of 10^{10} $cm^{-2}{\cdot}s^{-1}$. The analysis of V used a 600 s irradiation period and a 180 s decay interval, after which γ-ray spectra were acquired for 300 s each using an HPGe spectrometer. The analysis of O used cyclic (*n*=5) irradiations/counts of 20 s each. High-energy gamma radiation from the decay of ^{16}N was observed using a BGO spectrometer.

Hard X-ray photoelectron spectroscopy (HAXPES)

HAXPES measurements were performed at the National Institute of Standards and Technology beamline SST-2 of the National Synchrotron Light Source II of Brookhaven National Laboratory. Measurements were performed at approximately 2 keV photon energy with a pass energy of 200 eV and a step size of 0.85 eV with the analyzer axis oriented parallel with the photoelectron polarization vector. The higher excitation of HAXPES circumvents deleterious charging issues that are common to ultraviolet and soft X-ray photoelectron spectroscopy. Photon energy selection was accomplished using a double Si (111) crystal monochromator. No evidence of charging was observed during our measurements. The beam energy was aligned to the Fermi level of a silver foil before measurements.

X-ray Absorption Near Edge Spectroscopy

V *L*- and O *K*- XANES measurements were carried out at the National Synchrotron Light Source II of Brookhaven National Laboratory beamline SST-1 operated by the National Institute of Standards and Technology. Measurements were performed in partial electron yield (PEY) mode with a nominal resolution of 0.1 eV. The PEY signal was normalized to the incident beam intensity of a clean gold grid to eliminate the effects of any incident beam fluctuations and optics absorption features.

Extended X-ray Absorption Fine Structure

V K-edge EXAFS spectra were collected at the Advanced Light Source (ALS) bending-magnet beamline 10.3.2 (2.4–17 keV). The storage ring is operated at 500 mA and 1.9 GeV. Spectra were collected in fluorescence mode in the energy range 5350—6300 eV (up to k≈14.5 $Å^{-1}$) by continuously scanning the Si (111) monochromator. A Canberra 7-element solid-state detector with a Be window was used for data collection. V foil was used as the calibration standard. LabVIEW custom software was used to perform deadtime correction, glitch removal, energy calibration, pre-edge subtraction, and post-edge normalization.[17] The Athena suite of programs in the IFEFFIT package was used for further data analysis. Data in the k-range 2.25 $Å^{-1}$—9.75 $Å^{-1}$ was selected for fitting and Fourier transformed to obtain R-space data. The R-space data was then used to perform first-shell (V—O) fitting. Multishell least-squares parameter fitting of the V K-edge EXAFS data was performed using the ARTEMIS module of the IFEFFIT software package.[18] The photoelectron mean free path, scattering amplitude, and phase functions were calculated using the FEFF6 program.[19]

Table S1. Refined lattice parameters, atom positions, and thermal parameters for hydrothermally prepared Ge-doped VO_2

a = 5.75828(21)Å, b = 4.53020(29)Å, c = 5.38762(25)Å, β = 122.591(4)°, V = 118.412(4)$Å^3$ χ^2 = 2.717, wRp = 5.77%, Rp = 4.63%					
Atom	X	y	z	Occupancy	U_{iso} (10^2, Å)
V	0.23820(73)	0.97975(74)	0.02522(79)	0.9180	3.285(72)
O(1)	0.0899(21)	0.2086(18)	0.2032(20)	1.0000	2.12(32)
O(2)	0.4247(20)	0.7038(18)	0.3068(19)	1.0000	1.58(31)
Ge	0.23820	0.97975	0.02522	0.0820	3.285

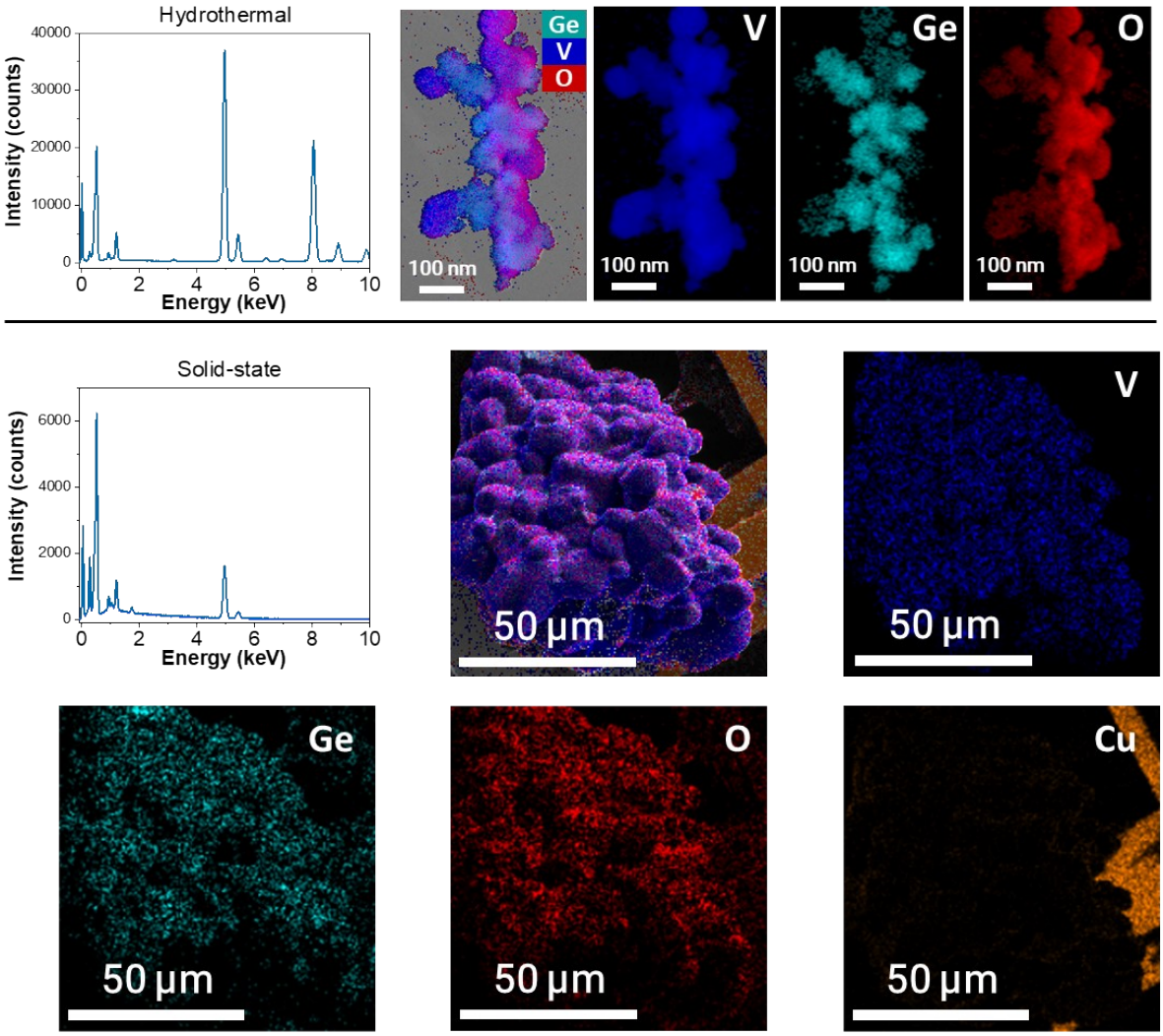

Figure S1. (Top) EDX maps collected for V, O, and Ge signals for the hydrothermally prepared $Ge_{0.02}V_{0.98}O_2$. (Bottom) EDX maps collected on solid-state-prepared $Ge_{0.04}V_{0.96}O_2$, with separated components for V, O, Ge, and Cu grid signals.

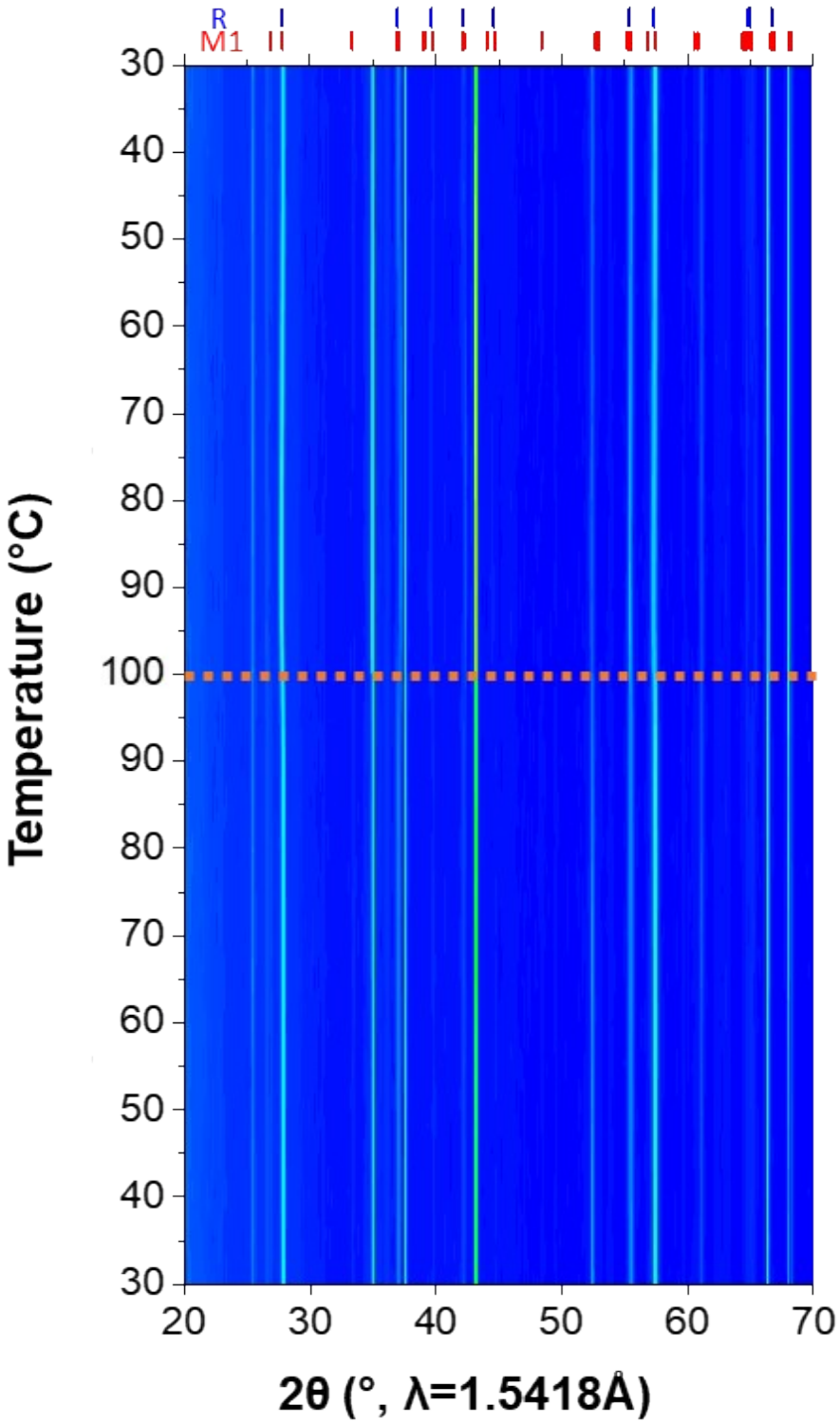

Figure S2. Temperature-dependent powder X-ray diffraction of hydrothermally prepared $Ge_{0.06}V_{0.94}O_2$. Full diffraction patterns were collected every 5°C increment from 30°C, increasing to 100 °C, and decreasing back to 30°C.

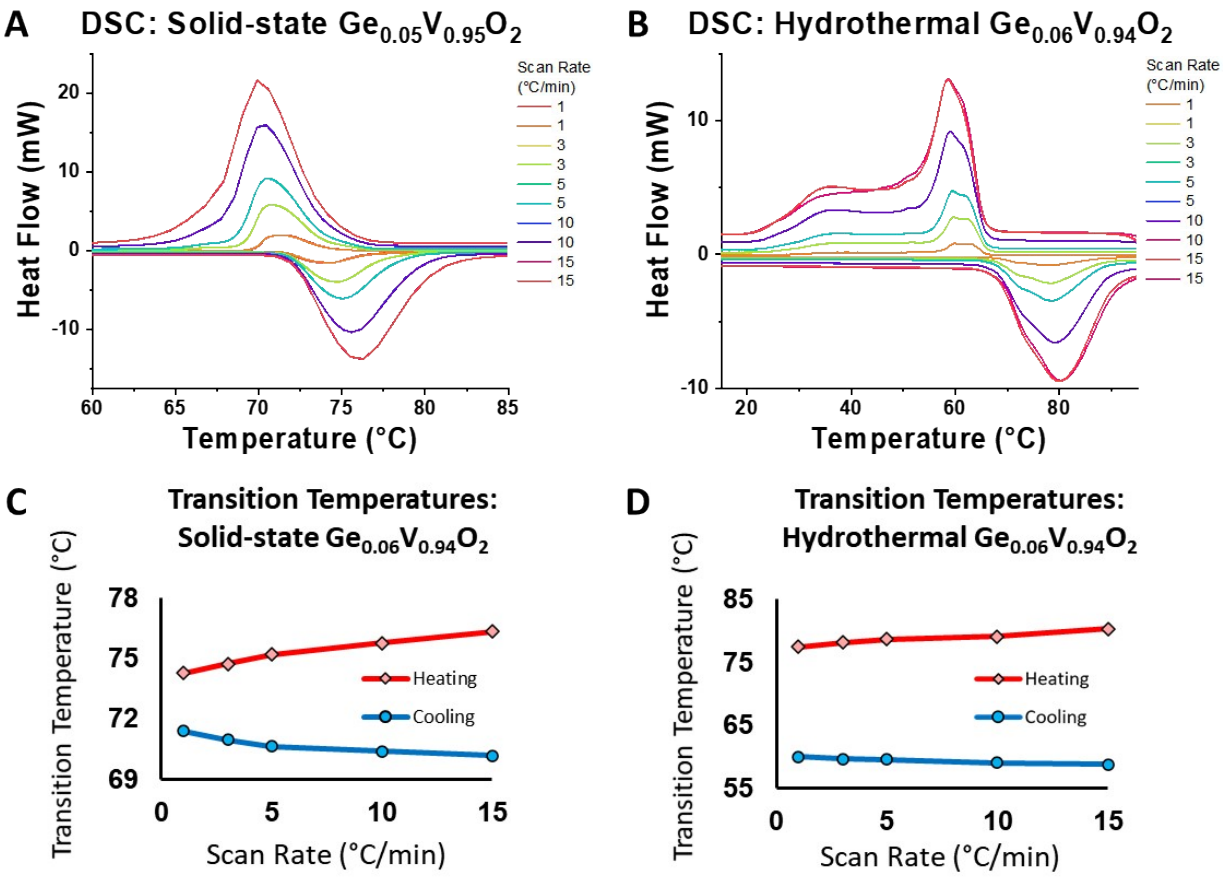

Figure S3. Rate-dependent differential scanning calorimetry of solid-state-prepared and hydrothermally prepared $Ge_xV_{1-x}O_2$. Scan rates studied were 1, 3, 5, 10, and 15 (°C/min). Generally, scan rate symmetrically expands hysteresis between heating and cooling transitions. There is no appreciable rate-dependence to either of the transition temperatures in either sample.

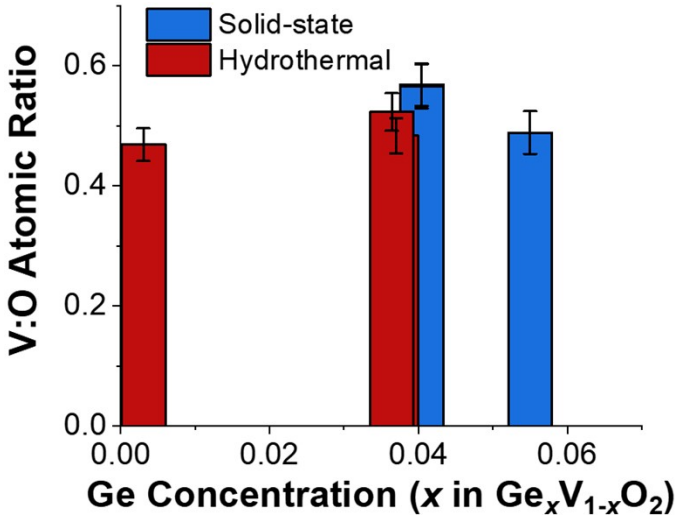

Figure S4. Oxygen-to-vanadium atomic ratios as measured by neutron activation analysis with error bars. Solid-state-prepared samples are shown in blue, whereas hydrothermally prepared samples are shown in red. The averages for each sample set are shown without colour immediately adjacent to their constituent members.

Table S2. DFT-derived bond distances for V-O polyhedron in undoped VO_2 and Ge-doped VO_2

Bond	Bond distance (Å)	
	Undoped VO_2	Ge-doped VO_2
V-V (short)	2.622(6)	2.613(5)
V-V (long)	3.167(5)	3.175(5)
V—O1	1.860(10)	1.899(8)
V—O1	1.869(10)	1.818(8)
V—O1	2.033(6)	2.034(5)
V—O2	1.746(6)	1.806(5)
V—O2	1.993(10)	1.930(7)
V—O2	2.131(10)	2.142(8)

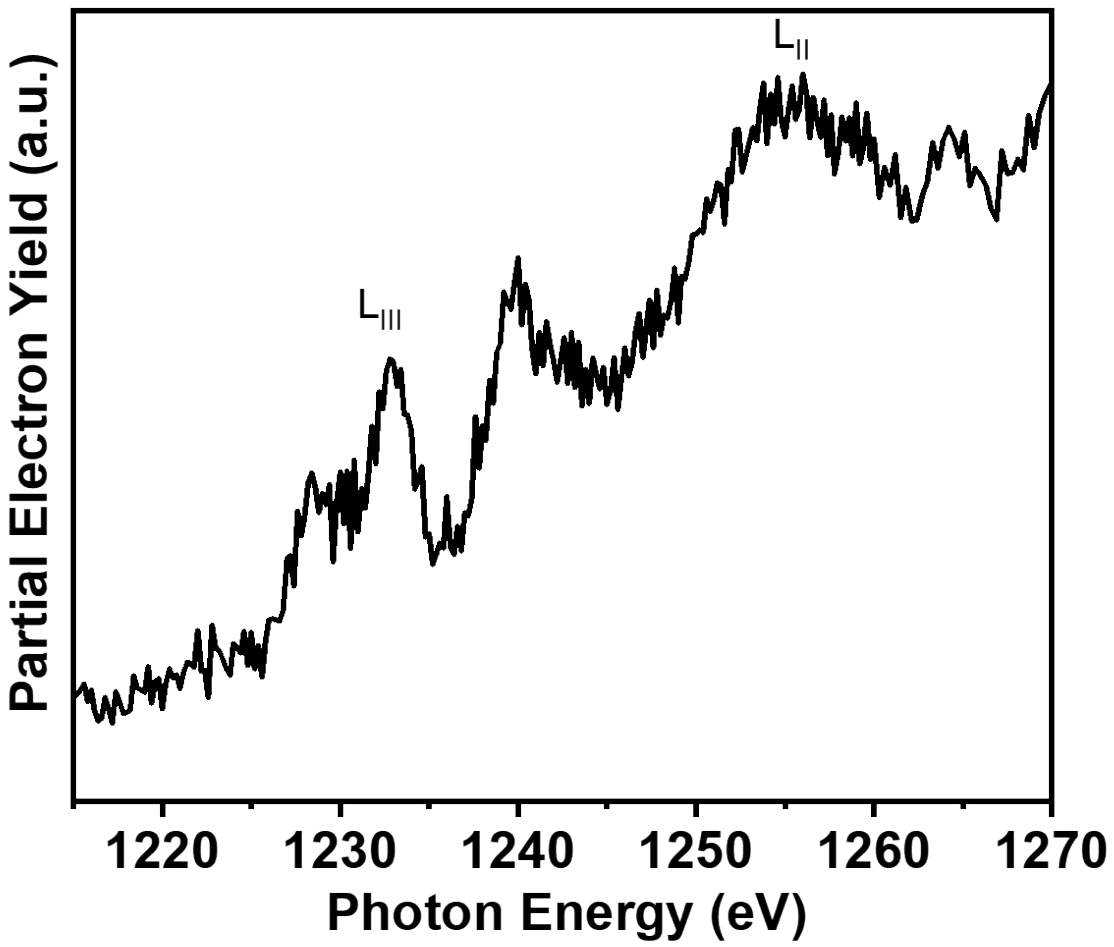

Figure S5. XANES spectrum of the Ge L_{II}- and L_{III} -edge in hydrothermally prepared $Ge_{0.06}V_{0.94}O_2$. The energy positioning of the Ge L-edge features suggest a chemical environment consistent with nominally tetravalent Ge. [20]

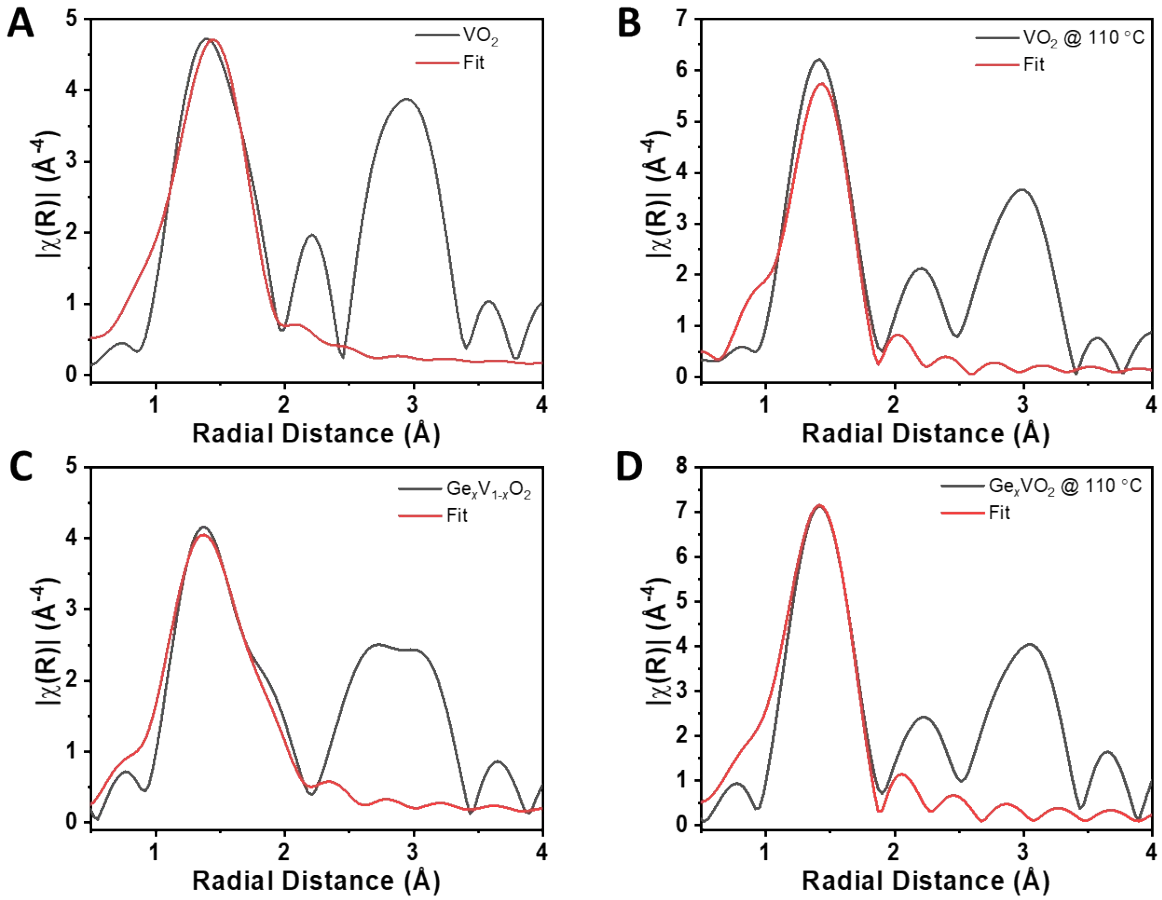

Figure S6. EXAFS first-shell data fittings for A: undoped VO_2 at room temperature. B: Unalloyed VO_2 at 110 °C. C: $Ge_{0.06}V_{0.94}O_2$ at room temperature. D: $Ge_{0.06}V_{0.94}O_2$ at 110 °C

Table S3. EXAFS-derived vanadium first-shell fitting data. Room-temperature data are fitted to structures in $P2_1/m$ symmetry while the data collected at 110 °C are fitted to $P4_2/mnm$ symmetry.

Sample	Path	N	*R* (Å)	σ^2* (Å²)	S_0^2**	ΔE_0 (eV)	*R*-factor***
VO_2 at room temperature	V-O1	1	1.873	0.011	0.8	-3.264	0.030
	V-O2	2	1.905	0.011			
	V-O3	2	2.003	0.011			
	V-O4	1	2.032	0.011			
VO_2 at 110 °C	V-O1	3	1.925	0.007	0.8	-4.396	0.029
	V-O2	3	1.949	0.028			
	V-O3	-	-	-			
	V-O4	-	-	-			
$Ge_{0.06}V_{0.94}O_2$ at room temperature	V-O1	1	1.866	0.007	0.8	-0.237	0.012
	V-O2	2	1.892	0.007			
	V-O3	2	2.048	0.007			
	V-O4	1	2.120	0.007			
$Ge_{0.06}V_{0.94}O_2$ at 110 °C	V-O1	3	1.881	0.009	0.8	-5.421	0.023
	V-O2	3	1.928	0.009			
	V-O3	-	-				
	V-O4	-	-				

* Mean square variation represents the uncertainty in a path length due to thermal and structural disorder.

** Amplitude reduction factor was kept constant at 0.8 for all four fits.

*** The R-factor for the fit is k-weighted (k1, k2, and k3).

References

1 L. Whittaker, H. Zhang and S. Banerjee, *J. Mater. Chem.*, 2009, **19**, 2968–2974.

2 B. H. Toby and R. B. Von Dreele, *Powder Diffr.*, 2014, **4814**, 2–6.

3 K. Momma and F. Izumi, *J. Appl. Crystallogr.*, 2011, **44**, 1272–1276.

4 K. Momma and F. Izumi, *J. Appl. Crystallogr.*, 2008, **41**, 653–658.

5 A. S. Barker Jr., H. W. Verleur and H. J. Guggenheim, *Phys. Rev. L*, 1966, **17**, 1286–1289.

6 P. Hohenberg and W. Kohn, *Phys. Rev. B*, 1964, **136**, 864–871.

7 W. Kohn and L. J. Sham, *Phys. Rev.*, 1965, **140**, 1133–1138.

8 G. Kresse and J. Furthmüller, *Phys. Rev. B*, 1996, **54**, 169–186.

9 J. P. Perdew, K. Burke and M. Ernzerhof, *Phys. Rev. Lett.*, 1996, **77**, 3865–3868.

10 D. C. Langreth and M. J. Mehl, *Phys. Rev. B*, 1983, **28**, 1809–1834.

11 H. J. Monkhorst and J. D. Pack, *Phys. Rev. B*, 1976, **13**, 5188–5192.

12 Y. Kumagai and F. Oba, *Phys. Rev. B*, 2014, **89**, 195205-1-195205–15.

13 A. V. Krukau, O. A. Vydrov, A. F. Izmaylov and G. E. Scuseria, *J. Chem. Phys.*, 2006, **125**, 224106-1-224106–5.

14 A. International, 2016, ASTM E385-16.

15 C. D. Fuerst and W. D. James, in *15th Intern. Conf. on the Application of Accelerators in Research and Industry*, Denton, TX, 1998.

16 E. P. Nargolwalla, S S Przybylowicz, *Activation Analysis with Neutron Generators*, John Wiley and Sons, New York, 1973.

17 W. Harris and G. N. White, in *Methods of Soil Analysis Part 5—Mineralogical Methods*, 2008, pp. 81–115.

18 B. Ravel, M. Newville and IUCr, *urn:issn:0909-0495*, 2005, 12, 537–541.

19 S. I. Zabinsky, J. J. Rehr, A. Ankudinov, R. C. Albers and M. J. Eller, *Phys. Rev. B*, 1995, **52**, 2995–3009.

20 F. Heigl, L. Armelao, X. H. J. Sun, C. Didychuk, X. T. Zhou, T. Regier, R. I. R. Blyth, P. S. G. Kim, R. A. Rosenberg and T. K. Sham, *J. Phys. Conf. Ser.*, , DOI:10.1088/1742-6596/190/1/012130.